Supporting Information for:

Exploring the Origin of the High Electro-Catalytic Activity for Nitrate-to-Ammonia Conversion on Electrodeposited Ni/Ru Hydroxide Hybrids

Fengling Zhou[a] and Chenghua Sun[b]

[a] Guangdong Provincial Key Laboratory of Distributed Energy Systems, Dongguan University of Technology, Dongguan, 523808, China. zhoufl@dgut.edu.cn
[b] Department of Chemistry and Biotechnology and Centre for Translational Atomaterials, Swinburne University of Technology, Hawthorn, VIC 3122, Australia. chenghuasun@swin.edu.au

Methods

Reagents. Sodium citrate (99%), Ruthenium chloride hydrate (35.0-42.0% Ru basis), potassium hydroxide (ACS), sodium hydroxide (97%) and n-butanol (99%) were purchased from Shanghai Aladdin Bio-Chem Technology Co. LTD. Salicylic acid (99%) and sodium hypochlorite solution (11-14% chlorine) were purchased from Alfa Aesar. Sodium nitroferricyanide dihydrate (99%) was purchased from Sigma-Aldrich. All the chemicals were used as received without any further purification. The nickel foam was purchased Changde Liyuan New Material Co., Ltd, and the weight density is 32 mg cm^{-2}. Milli-Q water (18 MΩ·cm) was used throughout the study.

Ru-LPD/pNF preparation: Partially oxidized Ru nanoparticles were synthesized using liquid phase deposition (LPD) method as detailed in the literature.[1] In detail, a solution of 0.6 g $NaBH_4$ in 20 ml of n-butanol was slowly added dropwise to a solution of 0.01 M $RuCl_3$ in n-butanol (40 ml) under continuous stirring. Then, 3 ml of H_2O was added and the solution was stirred for 180 min until no more bubble generated. The resulting precipitation was filtered and thoroughly rinsed with ethanol and ultrapure water, then dried in vacuum at 40°C for overnight.

To prepare the Ru-LPD/pNF electrode, a drop-casting method was used. A paste was prepared by mixing 5 mg of the Ru-LPD nanoparticles with 0.96 ml of H_2O-Ethanol mixture ($V_{H2O}:V_{Ethanol} = 3:1$) and 0.04 ml of 5% Nafion solution. The mixture was sonicated for 30 minutes, and then 10 µl of the paste was drop-cast onto a 0.25 cm^2 pristine nickel foam, which was then dried at 80°C in an oven for 2 hours. As a result, the electrode had a catalyst loading of 0.2 mg cm^{-2}.

Nickel foam treatment. The nickel surface are very easy to be oxidized in air, thus the nickel foam obtained were always coated with an oxidized layer by exposing and aging in air.

Pristine Nickel foam (pNF): the commercial nickel foam was washed with acetone, ethanol and ultrapure water with sonication, and then aged in air at ambient condition.

Reduced nickel foam (rNF): The above *p*NF was heat treated in a tube furnace at 400°C for 30 minutes under H_2 gas flow. The fresh *r*NF was used for electrodeposition immediately once taken out of the furnace.

Oxidized nickel foam (oNF): The above pNF was heat treated in a tube furnace in air at 300°C or 500°C for 30 minutes, and are labelled as oNF300 and oNF500, respectively.

Ru-Ni hybrid prepared by electrodeposition. The Ru-Ni hybrids were prepared by electrodeposition in a three-electrode system with the electrochemical work station CHI760. The electrolyte for deposition was consisted of 2g L^{-1} of $RuCl_3$ dissolved in 1.0 M HCl. Working electrodes were prepared using the above nickel foams with a surface area of 0.25 cm^2. The saturated calomel electrode (SCE) and the titanium foam were served as the reference and counter electrodes, respectively. All the voltage reported in this work were converted by referencing to the reverse hydrogen electrode (RHE) and can calculated by E (V) = E0 + 0.059*pH + 0.2415. In a typical electrodeposition, cycle voltammetry (CV) was applied on the NF in the voltage range of -0.4 V ~ 0.1 V vs RHE, at scan rate of 10 mV s^{-1}. The electrode prepared by 25 CVs on rNF, pNF, oNF300 and oNF500 were denoted as Ru-25CV/rNF, Ru-25CV/pNF, Ru-25CV/oNF300 and Ru-25CV/oNF500, respectively. After electrodeposition, the electrodes were thoroughly rinsed with ultrapure water and dried by nitrogen gas.

Electrochemical test. The electrochemical performances were investigated under ambient conditions using a three-electrode system controlled by an electrochemical station (CHI760). The saturated calomel electrode (SCE) and platinum foil were used as the reference and counter electrodes, respectively. All voltages reported in this work are converted with respect to the reversible hydrogen electrode (RHE). The working electrodes used for electrochemical tests and ammonia synthesis had surface areas of 0.25 cm^2. Cycle voltammetry (CV) was measured in 1.0 M KOH with 1.0 M $NaNO_3$ at a scan rate of 10 mV s^{-1}.

Electrochemical active area (ECSA). Cyclic voltammograms (CV) measured in aqueous 1 M KOH in the voltage range of 0.6 ~0.75 V at varying scan rates as shown in Figure S1a, and double layer capacitance (C_{DL}) calculated based on the CV data is shown in Figure S1b-d. The C_{DL} was calculated from Equation S1, using the charge (Q) from integrated area of the CV curve divided by the width of the potential window (ΔV). [2]

$$C_{DL} = dQ/dV = Q/\Delta V \qquad \text{(Equation S1)}$$

Then the electrochemical active surface area (ECSA) by calculated by Equation S2:

$$ECSA = C_{DL} / C_S \qquad \text{(Equation S1)}$$

Where Cs represents the capacitance of an ideal flat surface (a value of 40 μF/cm^2 was adopted in this study).[3]

Ammonia synthesis. Ammonia synthesis was conducted in an H-Cell with the counter and working electrodes separated by a glass frit. 50 ml of 1.0 M KOH with 1 M $NaNO_3$ was added into each part of the H-Cell. Saturated calomel electrode and platinum foil were used as reference electrode and the counter electrodes. Prior to electro-catalysis, the electrolyte was bubbled with Ar gas for 15 min to remove any reactive gases such as O_2, CO_2 and N_2. The electrolyte was continuously bubbled by Ar gas during the electro-catalysis. For nitrate-to-ammonia synthesis, a constant potential was applied on the working electrodes for 10 mins. The potentials ranged from -0.9 V to 0.2 V vs RHE to evaluate the potential effects.

In prolonged nitrate reduction, each part of the H-Cell was filled with 100 ml of 1 M KOH with 1.0 M $NaNO_3$. A constant potential of -0.2 V was applied on the working electrode for 100 hours continue electro-catalysis. During the long-term electro-catalytic reaction, the pH of the electrolyte in the cathode part will increases due to the products of OH^- ($NO_3^- + 8e^- + 6H_2O \rightarrow NH_3 + 9OH^-$). As the reduction potential shifts by $E = E^0 - 0.059pH$, the actual applied overpotentials drops due to the increased pH. Meanwhile, with continuing consumption of NO_3^-, its concentration will decrease, which also results in the current variation. To minimize these effects, a higher volume of electrolytes (100 ml) was applied for the long term electrolysis, and the electrolytes were renewed every 7 hours.

Ammonia detection. Ammonia detection was done using the indophenol blue method, as detailed previously. To reduce the effects of the ammonia contaminations, two strategies were applied. Firstly, the Ar gas was washed with 0.01 M H_2SO_4 to remove any NH_3 or NO_x in gas line before being plugged into the electrolytes. Secondly, for every UV-vis spectrum measurement, a blank spectrum were taken by using the same fresh electrolyte as the baseline. These strategies can eliminate the contamination imported from gas line system, and the environmental ammonia contaminations. The Faradaic efficiency was calculated based on the 8-electron process ($NO_3^- + 8e^- + 6H_2O \rightarrow NH_3 + 9OH^-$). The products were also analysed for the presence of nitrite, hydroxylamine and hydrazine, but no significant levels were found.

Materials Characterization. The morphology was characterized using scanning electron microscopy (SEM) on Zeiss Sigma 300. The more detailed morphology and the lattice spacing was obtained using a high-resolution transmission electron microscopy (HRTEM, FEI Talos F200) equipped with electron diffraction spectroscopy (EDS). The amounts of Ru on the electrodes were determined by Inductively Coupled Plasma Optical Emission Spectroscopy (ICP-OES) on Aglient 5110. The element states were analysed by X-ray photoelectron spectroscopy (XPS) on Thermo Fisher Scientific K-Alpha.

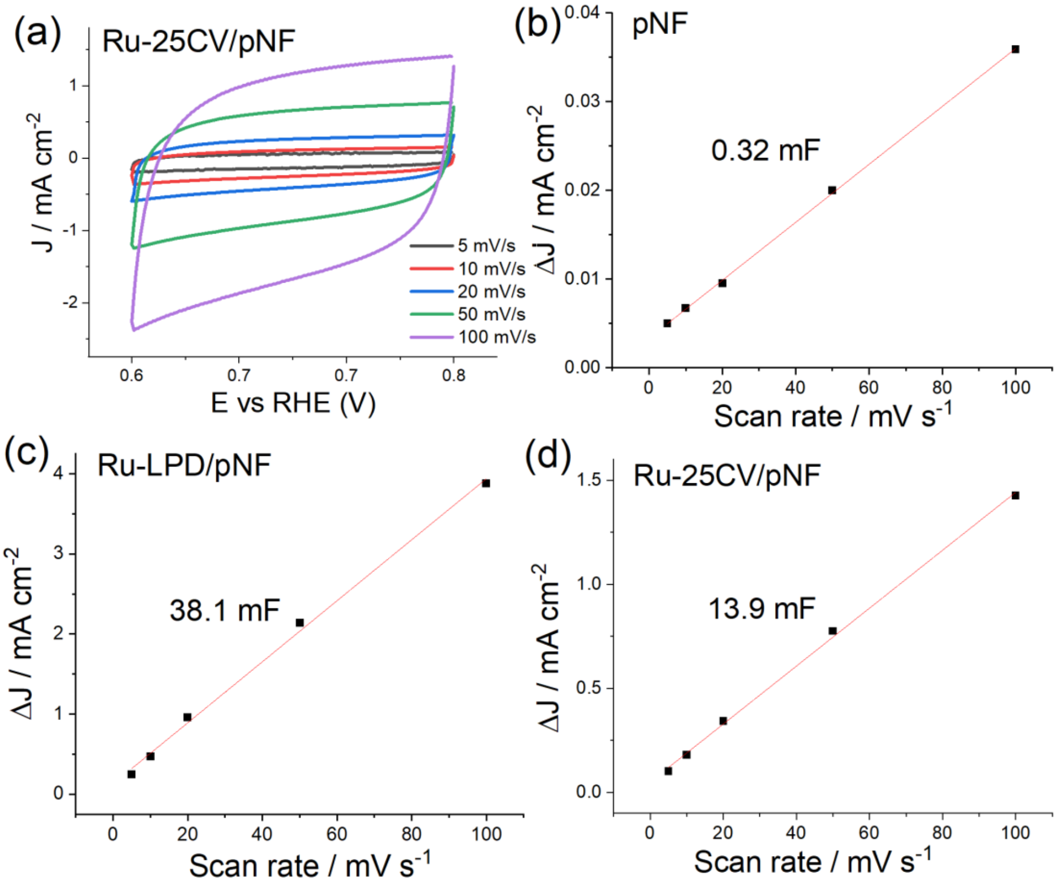

Figure S1. (a) Cyclic voltammetry of Ru-25CV/pNF (with a geometric area of 0.25 cm^2) measured in 1 mol L^{-1} KOH at room temperature at varying scan rates. (b-d) capacitance calculated based on the CV data

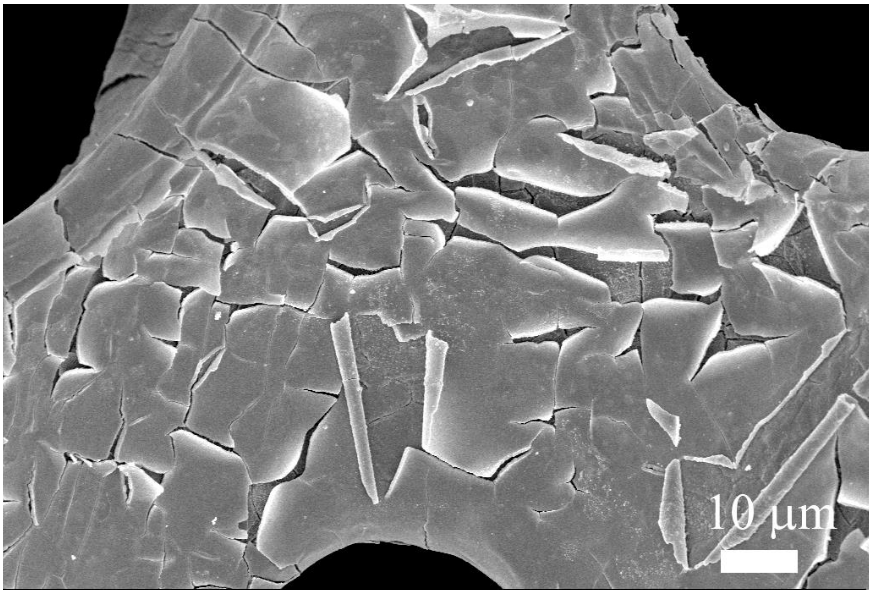

Figure S2. The SEM images of Ru-25CV/*p*NF

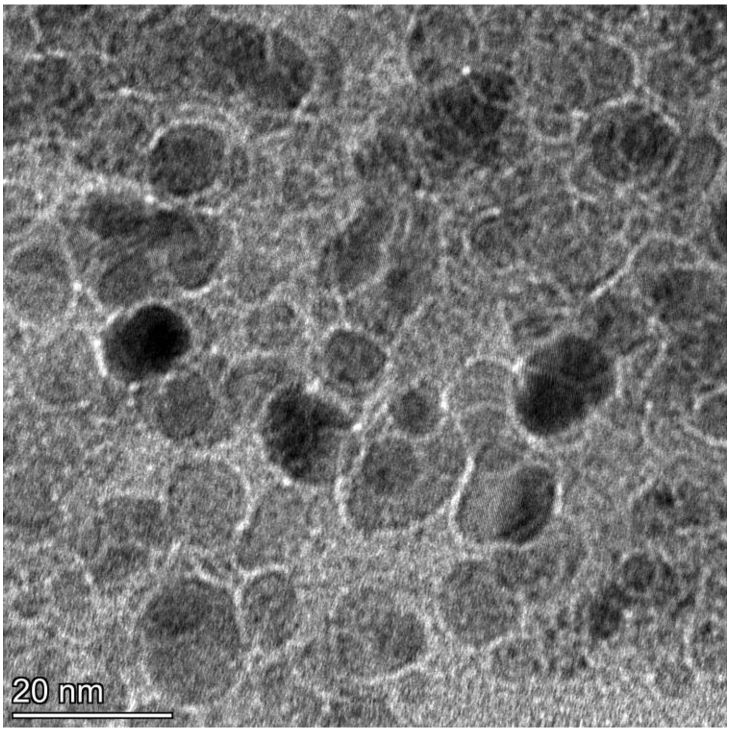

Figure S3. The TEM images of Ru-25CV/*p*NF

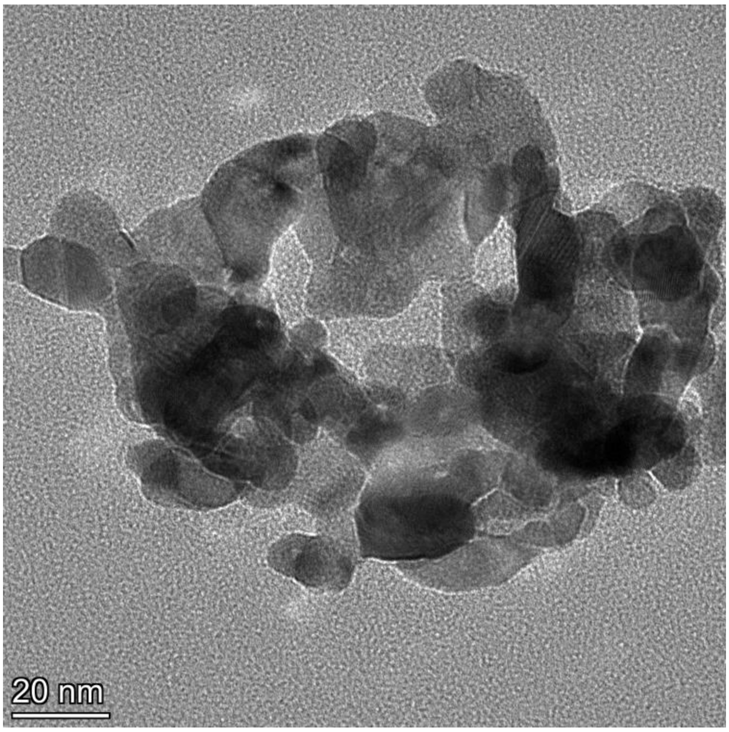

Figure S4. The TEM images of Ru-LPD

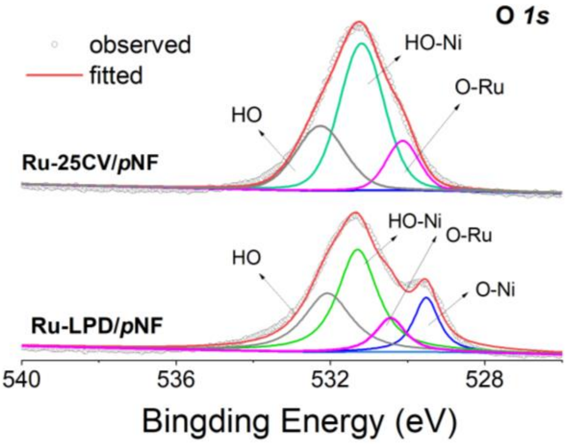

Figure S5.The XPS O 1s spectra of Ru-LPD/pNF and Ru-25CV/pNF.

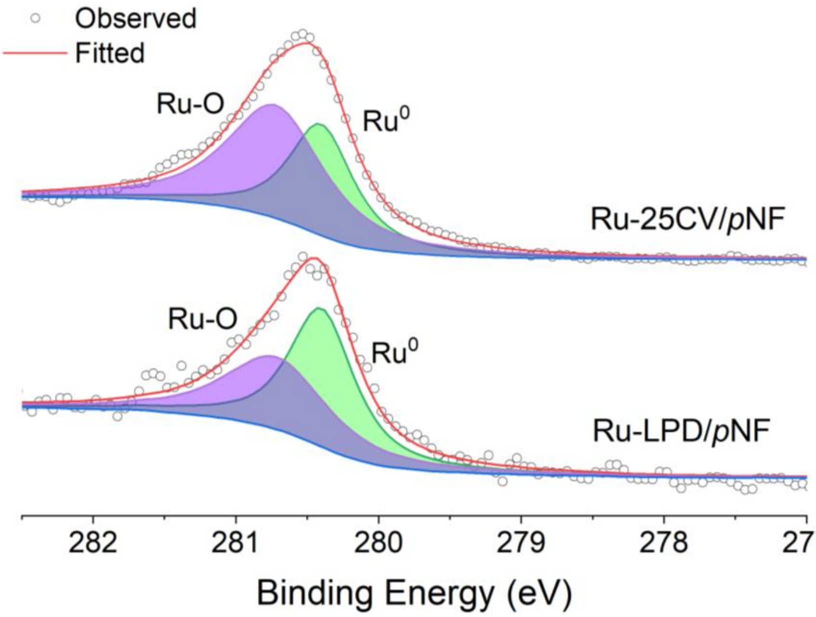

Figure S6.The XPS Ru 3d spectra of Ru-LPD/pNF and Ru-25CV/pNF.

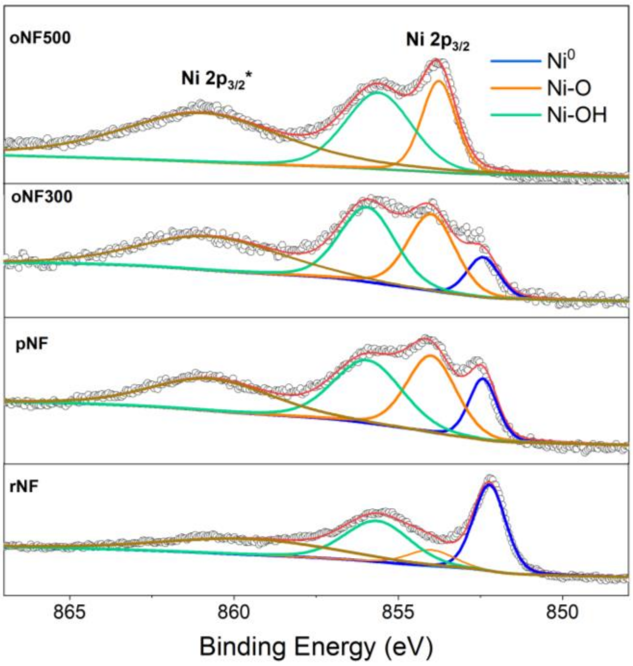

Figure S7. The XPS Ni 2p of the rNF, pNF, oNF300 and oNF500.

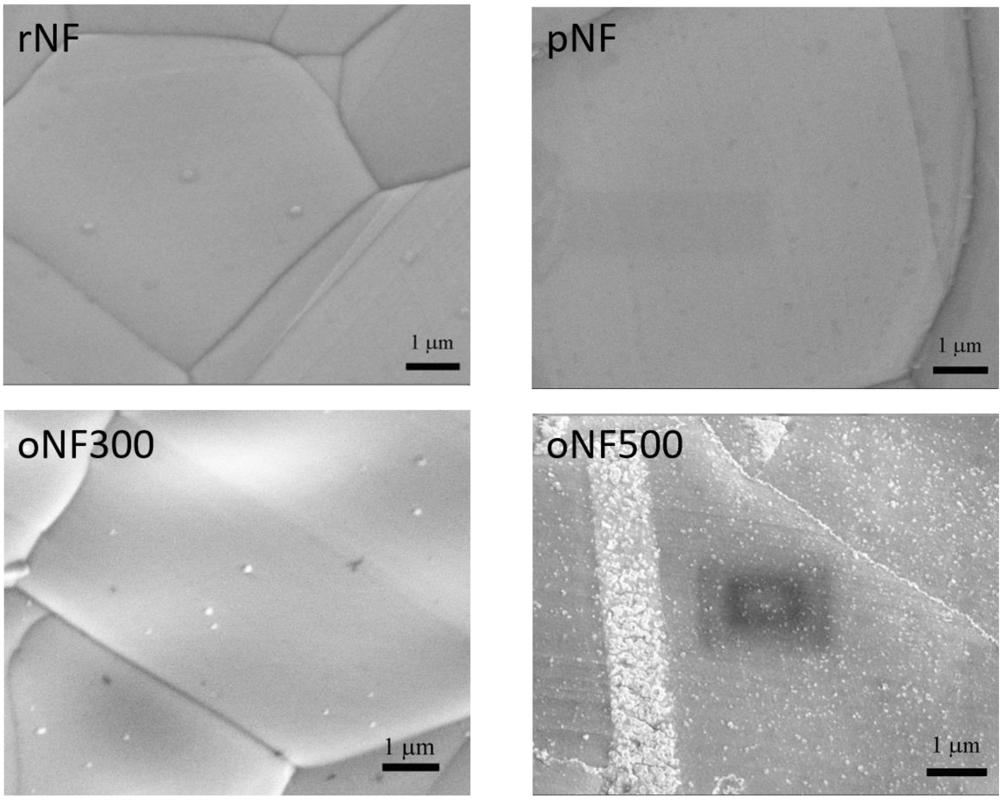

Figure S8. The SEM images of the pristine nickel foam (pNF), and reduced NF in H_2 flow (rNF) and oxidized NF in air (oNF300 and oNF500).

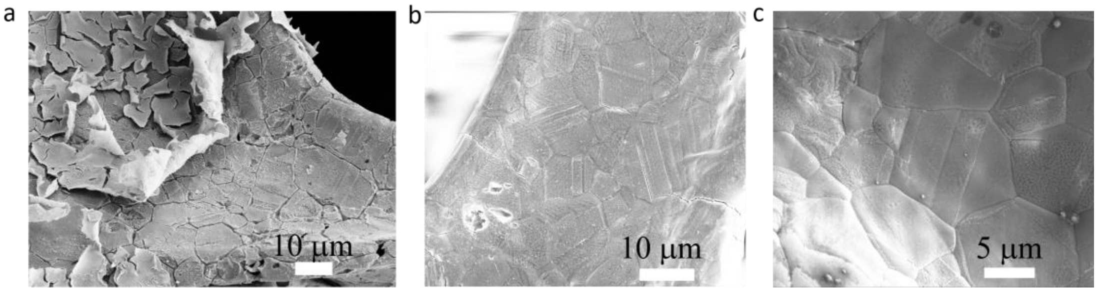

Figure S9. SEM images of Ru-Ni hybrids: (a) Ru-25CV/*r*NF, (b) Ru-25CV/oNF300, (c) Ru-25CV/oNF500.

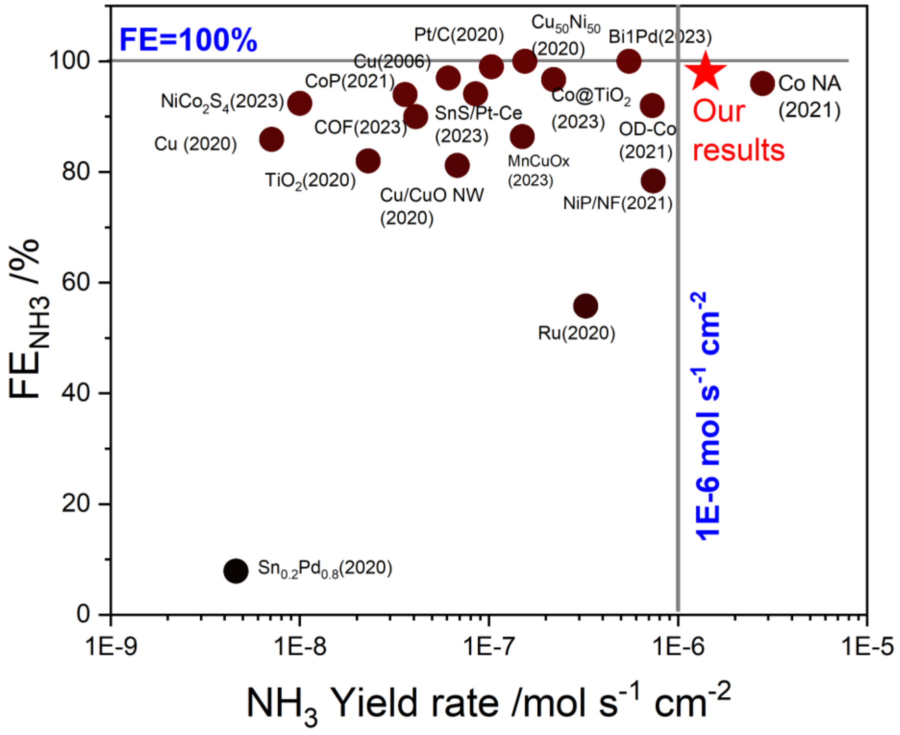

Figure S10. Comparison of ammonia selectivity and yield rate by electro-catalytic nitrate reduction.

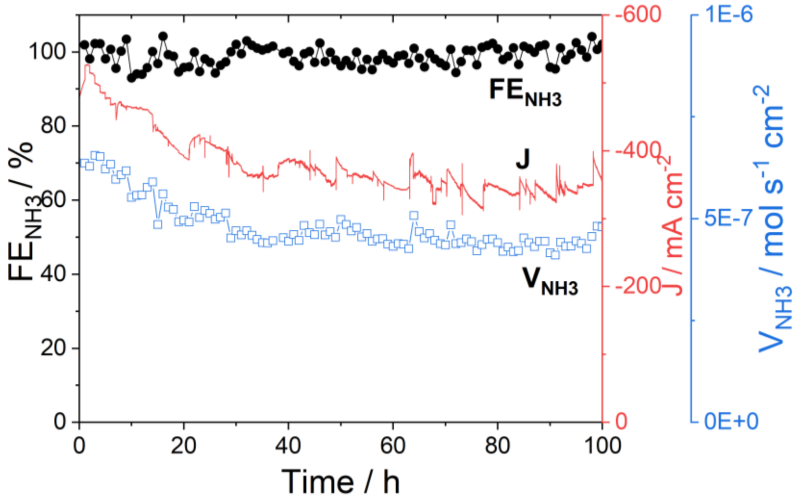

Figure S11. The current density, FE_{NH3} and the V_{NH3} under the applied potential of -0.2 V *vs* RHE during 100-hour electrocatalytic NITRR with electrolyte renewed every 7 hours.

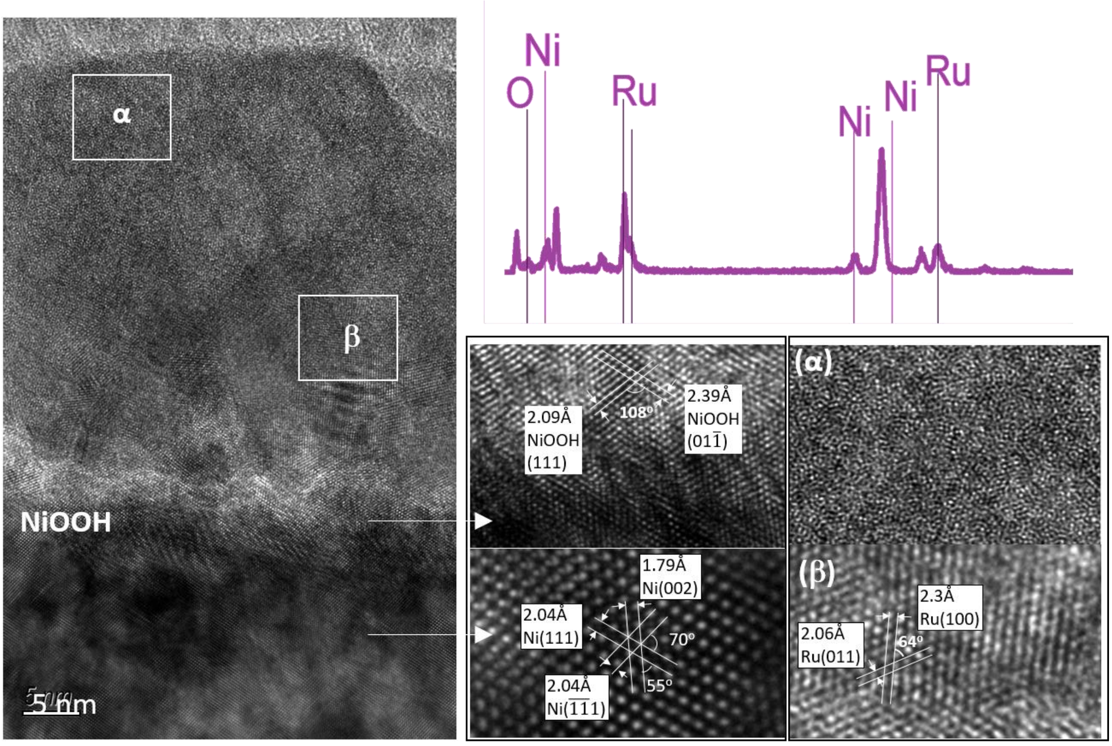

Figure S12. HRTEM images of Ru-25CV/oNF300.

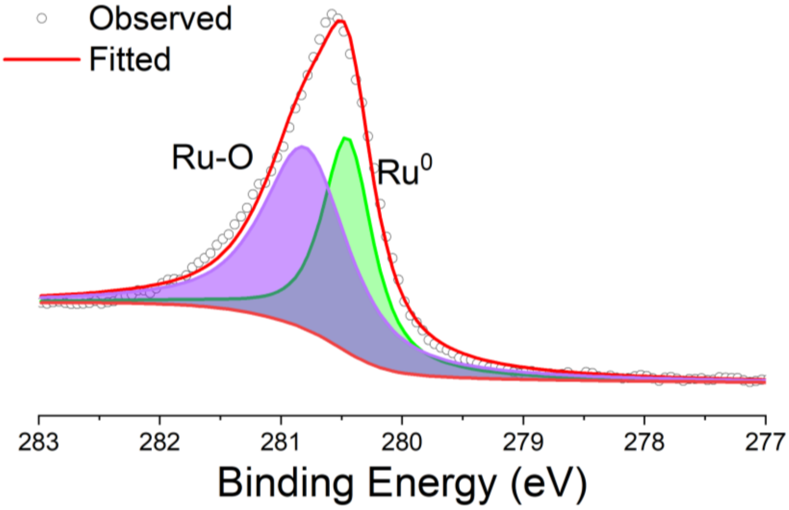

Figure S13.The XPS Ru 3d spectra of Ru-25CV/rNF.

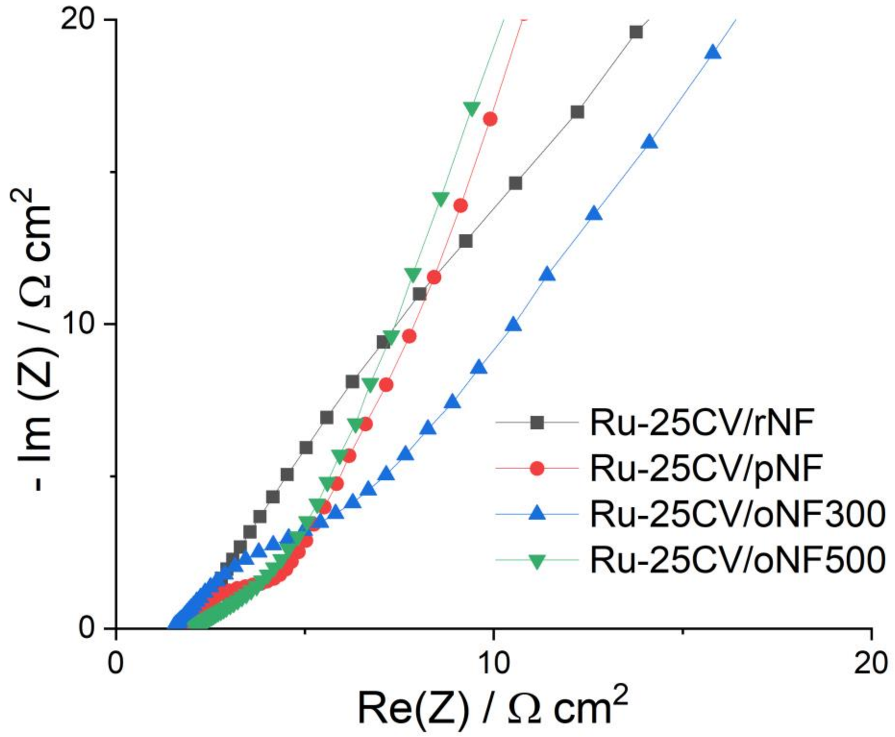

Figure 14. Impedance spectroscopy (Nyquist) of Ru-25CV on different substrates, measured in 1M NaOH.

References

1. Z. Ren, Y. Han, N. Cong, L. Jin, L. Tan, H. Chen, C. Zhai, X. Zhou, H. Fang and Y. Zhu, Hydrothermal synthesis of spherical Ru with high efficiency hydrogen evolution activity. *J. Electroanal. Chem.*, 2019. **848**,113320.
2. S. C. Pang, M. A. Anderson and T. W. Chapman, Novel electrode materials for thin-film ultracapacitors: Comparison of electrochemical properties of sol-gel-derived and electrodeposited manganese dioxide. *J. Electrochem. Soc.*, 2000. **147**, 444-450.
3. C. C. L. McCrory, S. Jung, I. M. Ferrer, S. M. Chatman, J. C. Peters and T. F. Jaramillo, Benchmarking Hydrogen Evolving Reaction and Oxygen Evolving Reaction Electrocatalysts for Solar Water Splitting Devices. *J. Am. Chem. Soc.*, 2015. **137**, 4347-4357.